Original Article

Formulation Development and Evaluation of Herbal Nanoparticles containing Ointment of Leaves extract of *Rhynchosia rothii*

Sharad D. Tayade[1,2]*, Narendra Silawat[1], Neetesh Jain[1]

[*1]Faculty of Pharmacy, Oriental University, Indore, Madhya Pradesh, India-453555;
[2]Department of Pharmaceutics, Rajarshi Shahu College of Pharmacy, Buldhana, Maharashtra, India-443001.

***Corresponding Author: -** Sharad D. Tayade

Email: sharad_tayade1@rediffmail.com
Doi: 10.47750/pnr.2022.13. S05.113

Abstract

In our previous work we have reported wound healing activity of leaves extract of *Rhynchosia rothii* in which we got excellent activity. Therefore in present study, the development of *Rhynchosia rothii* loaded Lycoat RS 720-BSA conjugated polymeric nanoparticles and subsequent ointment formulation has been aimed. Maillard Reaction was used to develop the Lycoat RS 720-BSA conjugate. The solvent evaporation approach was used to produce nanoparticles with *Rhynchosia rothii* loaded on them. The nanoparticles had a 257nm particle size and exhibited a spherical shape. The zeta potential in the formulation was -22.4 mV. Entrapment efficiency was 88.32% in the enhanced batch. The extracted content of the optimized batch was found to be 78.10%. A continuous release pattern was found by the *in-vitro* diffusion investigation, with 94.24% diffusion after 24 hours. The *Rhynchosia rothii* extract was created as an absorbent ointment formulation with a pH of 6.80–6.92 and a spread ability of 80.00–110.16 g.cm/s. It also has a distinctive aroma. Ointment containing herbal nanoparticles from the F4 batch has produced positive results. A new method of promoting nanoparticles in herbal medication delivery systems is by employing them in nanoparticles and an ointment. From present investigations we concluded that prepared ointment can be used clinically for the treatment of wounds if optimized further using more in vitro and in vivo models along with toxicity predictions.

Keywords: Herbal Nanoparticles, Lycoat RS-720, Solvent evaporation, Ointment, BSA

INTRODUCTION

For the treatment of skin conditions, a variety of topical dermatologic treatments, spanning from solids to liquids, are offered [1, 2]. The majority of ointments are made up of a base that primarily serves as a vehicle or carrier for the medications. The type of base also affects how well it works; therefore choosing an ointment base is a crucial step in formulation [3]. In contrast to fatty alcohols, traditional ointment bases have been oleaginous in nature, consisting of hydrocarbons like petrolatum, beeswax, and vegetable oils that do not permit the addition of any water. Topically applied ointments can serve a variety of functions, including protective, antimicrobial, emollient, antipruritic, keratolytic, and astringent. If the end product is to fulfill any of the aforementioned functions, the base of the ointment is crucial. The ointment base composition regulates the transfer of medications from the base to the human tissues as well as the depth of penetration [3, 4].

Particulate dispersions or solid particles with a size between 10 and 1000 nm are referred to as nanoparticles [5]. Their small size, variable composition, surface functionalization, and stability, which provide unique opportunities to interact with and target the tumor microenvironment, make them particularly alluring for the therapy of cancer [6, 7]. Polymeric nanoparticles are nanoparticles made of biocompatible and biodegradable polymers, either natural or manmade. Due to their small particle size and prolonged blood circulation, they have received specific attention during inspections for medication delivery and drug targeting [8].

The protein that is most abundant in plasma is BSA. It demonstrates significant buildup in the body's inflammatory and malignant regions [9]. It has a lengthy 19-day blood circulation half-life and several binding sites [10]. A serum albumin protein generated from cows is called bovine serum albumin. It is widely used as a benchmark for protein concentration. Lycoat RS 720 is a pea starch-based synthetic polymer. It exhibits strong film-forming and solution stability. It is the polymer with a regulated and sustained release [11, 12].

There are many species of *Rhynchosia* (Fabaceae) that are found in tropical and subtropical regions of the world. As an antibacterial, antidiabetic, abortive, healing, hepatoprotective, healer of boils, rheumatoid arthritis pain, and skin infection treatment, some plants from this genus have been utilized in traditional medicine [13]. So far, the genus *Rhynchosia* has yielded a total of 77 identified compounds, including as flavonoids, isoflavonoids, flavan-3-oils, xanthones, biphenyls, simple polyphenols, and sterols. Interestingly, prenylated C-glycosylflavonoids and isoflavonoids are abundant in the genus *Rhynchosia rothii* [13, 14].

In addition, nanoparticles have been used as a pharmaceutical medium for a number of years as part of the technology used in the manufacturing of herbal medicines. The microscopic shape of nanoparticles that will increase the compound solution and reduce the dosage of medication is one of the benefits of the nanoparticle technology. Additionally, nanoparticles maintain skin moisture, penetrate the skin, and improve skin stability [15]. Ointments are oil-based, semi-solid medications for external use that are simple to apply. Ointments shouldn't smell rancid; hence they should be made of oil or a fat emulsion or wax with high water content [16]. The objective of this research was to use the ionic glass process to create an ointment with a nanoparticle formulation that contained paraffin wax and *Rhynchosia rothii* extract. Various amounts of *Rhynchosia rothii* extract nanoparticles were combined with the ointment base.

MATERIALS AND METHODS

Rhynchosia rothii herb leaves were collected from near region of Buldhana in Maharashtra. We received a gift sample of bovine serum albumin (Fraction V) from HiMedia Pvt. Ltd. in Mumbai, India. The supplier of Lycoat RS 720 was Roquette Pharma Pvt. Ltd. in Mumbai, India. The sunflower wax was received from M/s Mahesh Ltd. in Mumbai, India as a gift sample. Analytical-grade compounds were utilized for all other substances.

Preparation of methanolic extract from leaves of *Rhynchosia rothii*

Researchers used the procedures listed below to produce the extract. 1.5 kg of dry plant leaf material were subjected to continuous methanol extraction in a Soxhlet thimble until the material was consumed. When the solvent has evaporated, the result is an amorphous dark green powder. Whattman No. 1 filter paper was used to filter this solution. A Rotary evaporator was used to evaporate the solvent under reduced pressure and 90°C, and the gummy extract was then stored at 4°C for later research [17].

Pharmacognostic and Qualitative phytochemical evaluation of plant extract

Using established techniques, the extracts of *Rhynchosia rothii* produced during the extraction process were subjected to pharmacognostic and preliminary phytochemical testing for the presence of several phytoconstituents. [17]

Compatibility study

On the DSC Lab: Mettler Instrument, the differential scanning calorimetry (DSC) thermograms of the pure extract and the improved formulation were captured. All samples (2-4 mg) were precisely weighed into standard aluminum pans for analysis, and then the pans were sealed with aluminum lids. Analysis was done between 0-350°C at a heating rate of 10 degrees per minute10°C/min in a nitrogen gas atmosphere (30 mL/min) [18].

FORMULATION AND DEVELOPMENT

Formulation of BSA-LYCOAT RS-720 conjugates

These Conjugates were prepared by Maillard reaction.

BSA and Lycoat RS 720 were dissolved together in water with a (1:1) molar ratio. The pH of the solution was adjusted to 7.1 with NaOH solution, then, the mixture solution was lyophilized. The lyophilized powder reacted at 60ºC and 79% relative humidity in a desiccator containing saturated KBr solution for 24 h. The resultant products were kept at -20ºC before use [19].

Nano preparation of extract

Polymeric nanoparticles were prepared by the solvent evaporation method. The polymeric nanoparticles were prepared by using plant extract to polymer conjugates ratio (1:2). The mixture was then subjected to Rotary evaporator for removal of the methanol. The dispersion is formed. It was subjected to high speed homogenizer (10,000 RPM for 15 min) and then passed through through high pressure homogenizer at pressure of 700 bars and 7 cycles. Nanoparticles solution subjected to lyophilization and dry lyophilized powder of herbal polymeric nanoparticles was formed [20].

Formulation of ointment

Oily Base Preparation: Paraffin wax is melted on a hot plate and liquid paraffin is added to it followed by preservative benzoic acid. The mixture was transferred to pestle and mortar and polymeric nanoparticle containing the plant extract was added and grinded at room temperature to obtain a fine paste like substance. The ratio of chemicals to be taken is optimized by hit and trial method. Flavoring agents were also added later.

FORMULATION DESIGN AND OPTIMIZATION OF BATCH:

Formulation Design

Different batches of herbal polymeric nanoparticles were prepared based on the 3^2 factorial designs. The independent variables were Polymeric conjugates concentration in terms of mg (X_1) and HPH pressure in terms of bar (X_2) for all formulation batches.

Optimization data analysis and model-validation

ANOVA was used to establish the statistical validation of the polynomial equations generated by Design Expert® Software. Fitting a multiple linear regression model to a 3^2 Factorial design give a predictor equation incorporating interactive and polynomial term to evaluate the responses:

$$Y = b0 + b1X1 + b2X2 + b12X1X2 + b11X12 + b22X22 \text{ ---------- (1)}$$

Where Y is the measured response associated with each factor level combination; b_0 is an intercept representing the arithmetic average of all quantitative outcomes of nine runs; bi (b_1, b_2, b_{11}, b_{12} and b_{22}) are regression coefficients computed from the observed experimental values of Y and X_1 and X_2 are the coded levels of independent variables. The terms X_1 X_2 represent the interaction terms.
Three dimensional response surface plots resulting from equations were obtained by the Design Expert® software [21].

CHARACTERIZATION OF BSA-LYCOAT RS-720 CONJUGATES AND HERBAL POLYMERIC NANOPARTICLES

Differential Scanning Calorimetry (DSC)

DSC was used to compare the DSC thermograms of BSA, Lycoat RS 720, and BSA-LYCOAT RS 720 at a heating rate of 10°C/min. The measurements were carried out in nitrogen atmospheres with a heating range of 30 to 250°C [22].

X-Ray Diffractometry (XRD)

Using an X-ray diffractometer with Cu as a target and a voltage of 40 kV, the powder X-ray diffraction (PXRD) patterns of BSA, Lycoat RS 720, and BSA-LYCOAT RS 720 were examined. Samples were examined at a scanning rate of 3o/2U/min in the 2θ angle range of 10-50ºC.

Particle size, Zeta potential and PDI analysis

Through the use of dynamic light scattering, the particle size and PDI were determined. By measuring Brownian motion and correlating it to particle size, dynamic light scattering (also known as PCS—Photon Correlation Spectroscopy) analyzes the movement of the particles. It accomplishes this by laser-illuminating the particles and examining the variations in light intensity in the scattered light. To create an acceptable scattering intensity, double distilled water was used to dilute all samples. Using disposable polystyrene cells with a 10 mm diameter and 25°C, the zeta potential and PDI values were measured at a 90° angle. By calculating the electrophoretic mobility, the zeta potential was calculated. For the optimized batch, the zeta potential and average particle size of the nanoparticles were calculated. (n = 3) [23].

Entrapment efficiency and Drug Loading

Nanoparticles dispersion was centrifuge at 12,000 rpm for 2 hrs, 1.0 mL of the supernatant collected after centrifugation was diluted with phosphate buffer pH7.4 and then makes up volume up to 10 ml in 10ml volumetric flask and measured. The pellets were re-dissolved in distilled water, and the supernatant was scanned with a UV-visible spectrophotometer in this parameter. The entrapment efficiency of the nanoparticles was calculated for each batch. The entrapment efficiency (EE %) in herbal polymeric nanoparticles was calculated from the following equation [24]:

$$\% \text{ EE} = \frac{\text{amount of drug added} - \text{amount of drug in supernatant}}{\text{amount of drug added}} \times 100 \text{ ---------- (1)}$$

Production Yield

The production yield of nanoparticles of various formulation were calculated using the weight of final product after drying with respect to the initial total weight of the extract and polymer conjugates used for preparation of polymeric nanoparticles [25].

$$\text{Production yield} = \frac{\text{Amount of freezed dried powder}}{\text{Amount of extract and Polymer in feed}} \times 100 \text{---------- (3)}$$

Surface Morphological Study

Surface morphology of the herbal polymer nanoparticles was performed by using transmission electron microscopy. A formulation (1mg/ml) was placed on Formvars coated copper grids and allowed to equilibrate. Excess liquid was removed with a filter paper and dried at room temperature for about half an hour. The dried grid containing the herbal nanoparticles was visualized using TEM [26].

In-vitro diffusion study

For the drug release studies, Franz diffusion cells were employed. Onto the cellulose membrane's surface, ointment was equally distributed. Between the donor and the receptor chambers of the diffusion cell, the cellulose membrane was clamped. Phosphate buffer with a pH of 7.4 was placed in the receptor compartment, and the assembly was kept at 37°C with intermittent magnetic stirring. The donor compartment membrane received 300 mg of ointment, which was subsequently wrapped in aluminum foil to prevent drying out. Over the course of one hour, aliquots were taken out at regular intervals for analysis using a UV spectrophotometer [27, 35].

Stability of Nanoparticle

The stability of the produced nanoparticles was evaluated by keeping the optimum formulation in a stability chamber (at 4°C) for three months. The particle size, zeta potential, entrapment efficiency and physical appearance were determined at different time intervals of one, two and three months (According to ICH Q1A) [28-30].

EVALUATION OF OINTMENT

Organoleptic characteristics

Physical appearance, color, texture, phase separation, and homogeneity tests were performed on all blank formulations (i.e., formulations devoid of an active component) and extract-loaded formulations. Visual observation was used to assess these qualities. By pressing a tiny amount of the prepared ointment between the thumb and index finger, homogeneity and texture were evaluated. The texture and homogeneity of the formulations were assessed using the formulations' consistency and the presence of coarse particles. Also assessed was the immediate skin feel (including stiffness, grit, and greasiness) [31].

Water number

The greatest amount of water that can be added to 100 g of base at a specific temperature is known as the water number. It was discovered by adding distilled water while mixing the base continually. The amount of water still in the container was considered the end point when no more water could be absorbed into the base as shown by water droplets.

pH

In a dry beaker, 2.5 g of each formulation was added together with 50 ml of water. Ointments were cooked in a beaker on a water bath at 60 to 70°C. Using a pH meter, determine the ointment's pH (pH Tutor, Eutech Instruments). The calculations were done three times, and the averages of the three measurements were recorded [32].

Spreadability

An instrument suggested by Multimer was modified to measure the spreadability of the formulation. It is made up of a wooden block with a pulley attached to one end and a fixed glass slide on the other. a 3g overabundance of cream applied on a ground plate. Between this plate and a second glass plate with the dimensions of a fixed ground plate and a hook, the ointment was sandwiched. To remove air and create a consistent film of ointment between the plates, a 1 kg weight was set on top of the two plates for five minutes. The borders were scraped clean of extra ointment. Next, a 240 g pull was applied to the top plate. The top plate's time to travel a distance of 10 cm was measured with the aid of a spring attached to the hook. Better Spreadability is indicated by a shorter interval [33]. In order to determine spreadability, the following formula was used:

$$S = M \times L/T$$

Where, S = Spreadability
M = Weight in the pan (tied to the upper slide)
L = Length moved by the glass slide and
T = Time (in seconds) taken to separate the slide completely each other.

Viscosity

Rheological tests were conducted using a Brookfield Synchro-Lectric Viscometer (Model RVT) with a Helipath Stand. Before measuring the dial reading with a T-D spindle at 10, 20, 30, 50, 60, and 100 rpm, the sample (50 g) was put in a beaker and allowed to equilibrate for 5 min. The dial reading on the viscometer was recorded for each speed. The dial reading that corresponded to each decrease in spindle speed was recorded. At room temperature, the measurements were made in triplicate. The viscosity in centipoises (CPS) was obtained by directly multiplying the dial readings by the coefficients listed in the Brookfield Viscometer catalog [34].

Stability testing

According to the International Conference on Harmonization (ICH) criteria, a stability analysis of the developed ointment formulations was conducted. The prepared ointment was placed in collapsible tubes, stored for three months at three different temperatures and humidity levels 25°C±2°C/60%±5% RH, 30°C±2°C/65%±5% RH, and 40°C±2°C/75%±5% RH respectively and then its appearance, pH, viscosity, and spreadability were examined [36, 37].

RESULT AND DISCUSSION

Method of extraction

The methanol is used as organic solvent for the extraction process. The extract (100g) was refluxed with the methanol. The solvent from the extract were removed under a vacuum. The extractive value was calculated by weighing. The sample was stored at 4ºC. The extraction value for the plant in methanol is given in Table 1.

Table 1. Pharmacognostic parameter of extract

Solvent	Value (g)
Methanol soluble extractive values (%w/w)	15.2
Total ash value (%w/w)	7.5%
Acid insoluble ash value (%w/w)	0.7%
Water soluble ash value (%w/w)	3.2%
Foreign organic matter (%w/w)	0.5%
Moisture content (%w/w)	0.220%
Loss on drying (%w/w)	3.9%

Qualitative phytochemical screening of plant extract

The curative properties of medicinal plants are perhaps due to the presence of various secondary metabolites such as alkaloids, flavonoids, glycosides, saponins, tannins, triterpenes, sterols *etc*. Thus the preliminary screening tests may be useful in the detection of the bioactive principles and subsequently may lead to the drug discovery and development. Further, these tests facilitate their quantitative estimation and qualitative separation of pharmacologically active chemical compounds.

Preliminary phytochemical screening with various qualitative chemical tests revealed the presence of alkaloids, tannins, flavonoids, proteins, and mucilages present in the *Rhynchosia rothii* leaf extracts and Glycosides, saponins, and amino acid were absent in the *Rhynchosia rothii* leaf extracts as per given in Table 2.

Table 2. Qualitative phytochemical screening of plant extract

Test performed	Observation
Tests for Carbohydrates (Molish Test)	-
Test for Monosaccharide (Barfoed's Test)	-
Test for Non-reducing polysaccharides (Iodine Test)	-
Test for Proteins (Biuret test, Millions test)	+
Tests for Steroids (Libermann Burchard reaction)	-
Tests for Terpenoids	-
Test for Saponin (Foam test)	-
Tests for Flavonoids (Shinoda test)	+
Tests for Flavonoids (Ferric chloride test, Lead ethanoate test, Sod-hydroxide Test)	-
Test for Tannins & Phenolic compounds ($FeCl_3$ Lead acetate)	+
Test for alkaloids (Mayer's reagent)	+
+ Indicates presence of phytoconstituents, - Indicates absence of phytoconstituent	

Compatibility study

The improved formulation F6 and pure extract underwent DSC analysis. Pure extract and the improved formulation both had separate melting endotherms at 313.41°C and 162.65°C, respectively, with enthalpy values of -51.93 J/g and -168.44 J/g. Thermograms of the pure extract and optimal formulation chosen for the investigation are shown in Figs. 1-2. No peak was seen in the region of 313.41°C in the formulation (F6) Fig. 2 example, confirming the drug's molecular dispersion in the polymer matrix and trapping inside the polymeric nanoparticles. Most of the time, the medicines' melting endotherm was well preserved. In all instances of optimal formulation, the drug's melting endotherm was well conserved with little to no change in enthalpy value, showing the drug's compatibility with the study's selected excipients.

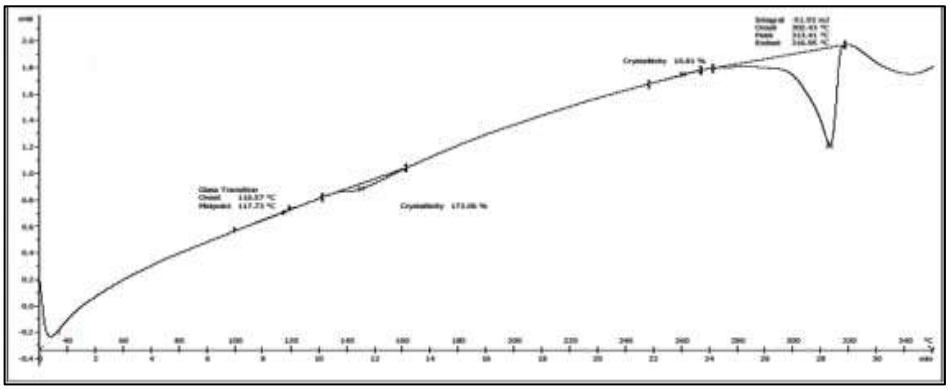

Fig. 1. DSC of Pure Extract

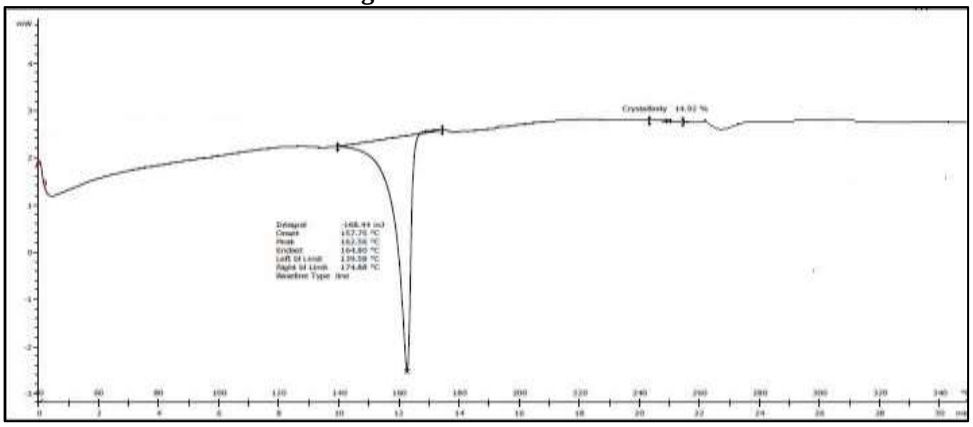

Fig. 2. DSC of Optimized Formulation (F6)

FORMULATION AND DEVELOPMENT

Formulation Design and Optimization of Batch

Formulation Design

Various Formulation batches of Herbal Polymeric nanoparticles were prepared based on 3^2 factorial designs. The independent variables were Polymer conjugates concentration in terms of mg (X_1) and HPH pressure in terms of bar (X_2) and their levels are shown in table 1 MPS i.e. Mean Particle Size (d.nm) (Y1) and Entrapment Efficiency (%)(Y2), were taken as response parameters as the dependent variables.

Table 3. Design Batches of Herbal Nanoparticles contain Extract

Formulation Code	X1 (mg)	X2 (Bar)	Y1 (d.nm)	Y2 (%)
F1	10	800	430	80.5
F2	10	800	450	80.9
F3	**40**	**500**	**329**	**86.6**
F4	40	300	377	87
F5	20	500	343	85.32
F6	**20**	**500**	**257**	**88.32**
F7	10	300	390	87.32
F8	20	800	456	80
F9	40	500	325	87

OPTIMIZATION DATA ANALYSIS AND MODEL-VALIDATION

A) Fitting of data to model

The two factors with lower, middle and upper design points in coded and un-coded values are shown in Table 3. The ranges of responses Y1 and Y2 were 255-715 d.nm and 80-89% respectively. All the responses observed for nine formulations prepared were fitted to main effect model, which was found as the best fitted model for Y1 and Y2, using Design Expert® software. The values of R2, adjusted R2, predicted R2, SD and % CV are given in (Table 4), along with the regression equation generated for each response. The results of ANNOVA in (Table 5), for the dependent variables demonstrate that the model was significant for all the response variables. It was observed that independent variables X1 (mg) and X2 (bar) had a positive effect on the entrapment efficiency and a desired particle size of nano-formulation i.e. nanoparticles was achieved.

Table 4. Summary of results of regression analysis for responses Y1 and Y2

Models	R^2	Adjusted R^2	Predicted R^2	SD	%CV
Response (Y1) Main Effect	0.8834	0.7668	0.6595	31.92	8.56
Response (Y2) Main Effect	0.9438	0.8875	0.8723	1.12	1.32

Regression Equations

$$Y1= +374.11+17.67*A[1]-22.33*A[2]-1.78*B[1]-51.78*B[2] \quad (8)$$

$$Y2= +84.76+0.21*A[1]-0.093*A[2]+2.35*B[1]+2.15*B[2] \quad (9)$$

B) Model Assessment for Dependent Variables:

After putting the data in Design Expert® software for, Fit summary applied to data in that Main Effect Model had been suggested by the software for all the responses. The statistical evaluation was performed by using ANNOVA. Results are shown in (Table 5). The coefficients with more than one factor term in the regression equation represent interaction terms. It also shows that the relationship between factors and responses is not always linear. When more than one factor are changes simultaneously and used at different levels in a formulation, a factor can produce different degrees of responses.

Table 5. Results of Analysis of Variance for Measured Response

Source of Variation	Sum of Square	DF	Mean of Square	F Value	p-value Prob> F	Summary Significant
Model (MPS)	30891.33	4	7722.83	7.58	0.0376	**Significant**
X1-Polymar Conc. (mg)	813.50	2	406.75	0.40	0.6950	
X2-HPH Press. (bar)	3963.00	2	1981.50	1.94	0.02571	
Model (EE)	83.68	4	20.92	16.78	0.0091	**Significant**
X1-Polymar Conc. (mg)	0.052	2	0.026	0.021	0.9796	
X2-HPH Press. (bar)	35.25	2	17.63	14.14	0.0154	

C) Response Surface Plot Analysis

Three dimensional response surface plots were generated by the Design Expert® software are presented in (Fig.3 and Fig.4) for the studied responses, i.e. Mean Particle Size (Y1) and Entrapment Efficiency (Y2). Fig.17 depicts response surface plot of Polymer Conjugate Concentration (X1) and HPH Pressure (X2) on Mean Particle Size. Nanoparticles being nanoparticulated structures, formulation batch amongst all the design batches giving least particle size will be preferred more and selected as an optimized batch. Where F6 Design Batch, with a polymer concentration of about 20 mg and HPH pressure 500 bar, shows the least particle size i.e. 257 nm.

Fig. 4 depicts response surface plot of Polymer Conjugate Concentration (X1) and HPH Pressure (X2) on entrapment efficiency. The 3-D surface image shows a linear response, which indicates with the increase in the polymer concentration the entrapment efficiency increases, as more the polymer available more will be the entrapment efficiency.

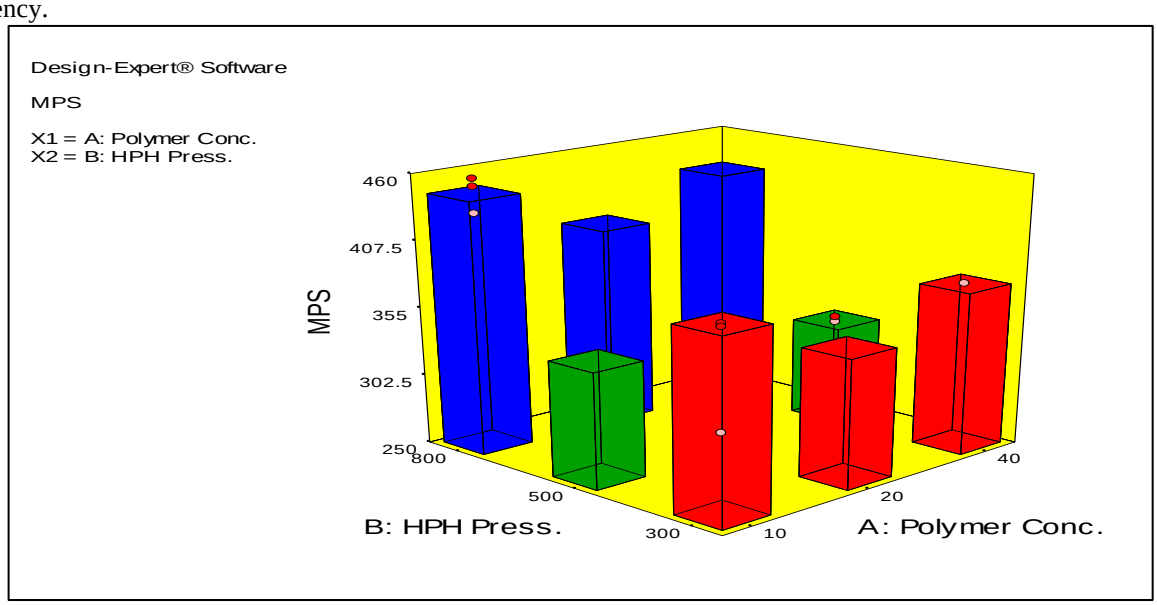

Fig. 3. Response surface plots for X1 and X2 on Mean Particle Size (Y1), where X1= Polymer Conjugates Concentration and X2= HPH Pressure

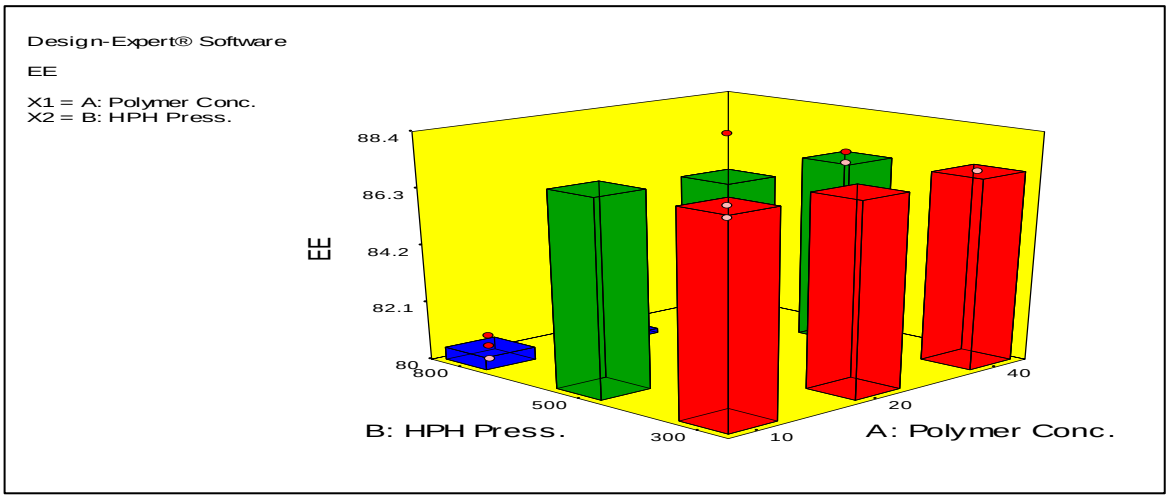

Fig. 4. Response surface plots for X1 and X2 on Entrapment Efficiency (Y1), where X1= Polymer Conjugates Concentration and X2= HPH Pressure

D) Optimisation of Result

The Optimization was performed on the basis of response surface modelling by using the numerical and graphical optimization model. Desirability is an objective function that ranges from zero outside of the limits to one at the goal. The numerical optimization finds a point that maximizes the desirability function. The Characteristics of a goal may be altered by adjusting the weight or importance. For several responses and factors, all goals get combined into one desirability function. The goal of optimization is to find a good set of conditions that will meet all the goals.

In case of Response Surface Graph for X1 and X2 on Mean Particle Size it is observed that considering the Polymer Concentration (X1) as the Polymer Concentration increases, more amount of drug is being incorporated into the nanoparticles and so the particle size reduces. In case of HPH pressure (X2) particle size found least at intermediate value i.e. 500 bars that indicate particle size 257 nm. But as there are two response factors so we cannot conclude the selection of Optimized batch based on just one response surface.

So, now considering the second Response surface graph for X1 and X2 on entrapment efficiency it was observed that as the polymer concentration increases the entrapment efficiency increases accordingly. Here two design batches i.e. F6 and F7 show maximum entrapment efficiency i.e. 88.32% and 87.32% respectively as show in Table 6. But as seen in first response Surface graph being a nanoparticle formulation considering the least particle size is also a crucial factor. So, the Design Batch with least particle size and maximum entrapment efficiency is selected. Therefore, F6 is considered as an optimised Batch.

Table 6. Optimization Result

Parameters	Lower Limit	Upper Limit	Goal	Solution
X1	10	40	In Range	20
X2	500	800	In Range	500
Y1	250	500	In Range	257
Y2	80	89	In Range	88.32

Formulation Of Ointment

Different formulations were made to optimize the composition of the ointment base and it was found that 1:3 ratio of paraffin wax: liquid paraffin showed the best consistency over the other ratios (1:1, 1:2, 2:1) as shown in Table 7.

Table 7. Formulation of ointment batches

Formulations	Hard Paraffin (g)	Liquid Paraffin (ml)	Preservative Benzoic acid (µl)	(Optimized F6) Plant Extract (ml)
F1	10	5	100	1
F2	5	5	100	1
F3	5	10	200	1
F4	10	30	300	2

CHARACTERIZATION OF BSA-LYCOAT RS 720 CONJUGATES AND NANOPARTICLES

Differential Scanning Calorimetry (DSC)

In Fig. 5, 6, and 7, DSC Thermogram of BSA and LYCOAT RS 720 showed sharp endothermic peak at 31.54ºC and 77.18ºC respectively, indicating crystalline nature. However, the both BSA and LYCOAT RS 720 peaks were disappeared in the conjugate with appearance of new peaks at 156.36ºC indicating compound BSA-LYCOAT RS 720 conjugate.

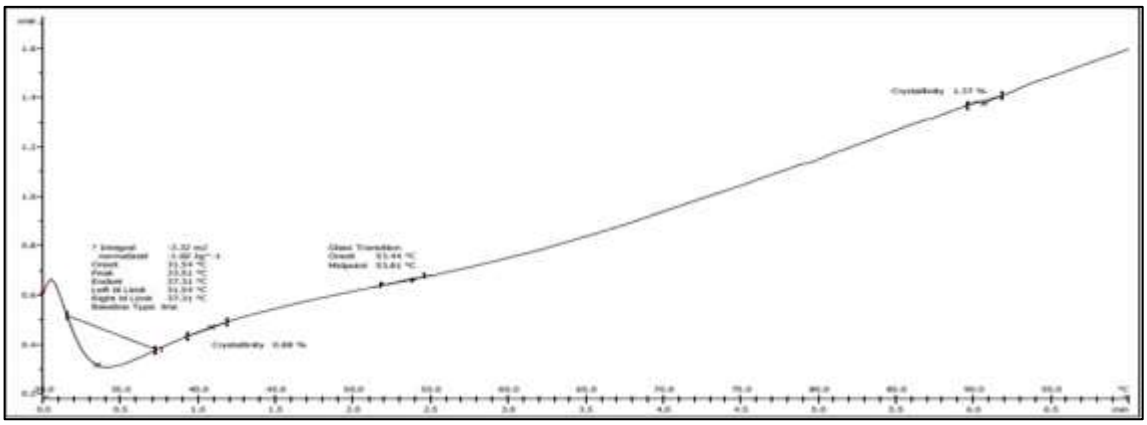

Fig. 5. DSC Thermogram of BSA

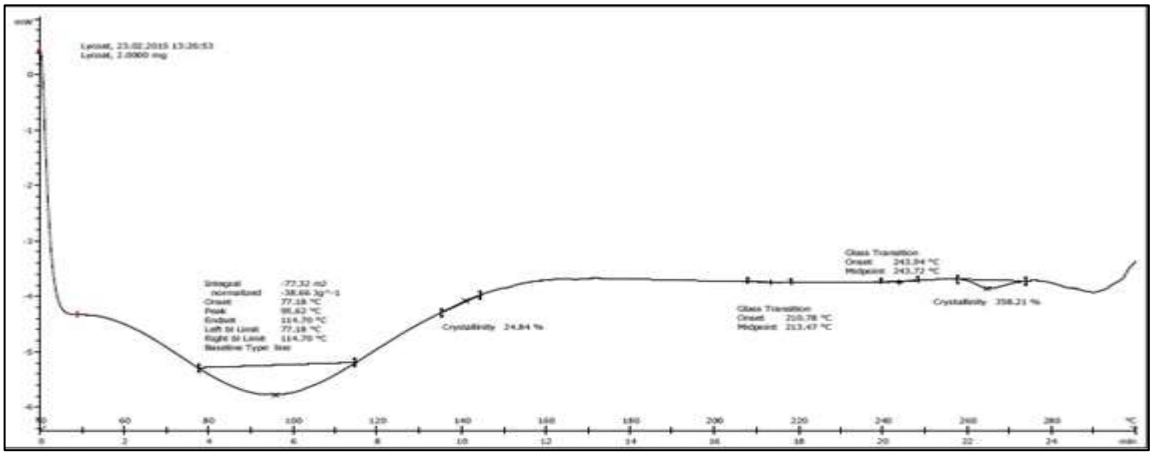

Fig. 6. DSC Thermogram of LYCOAT RS 720

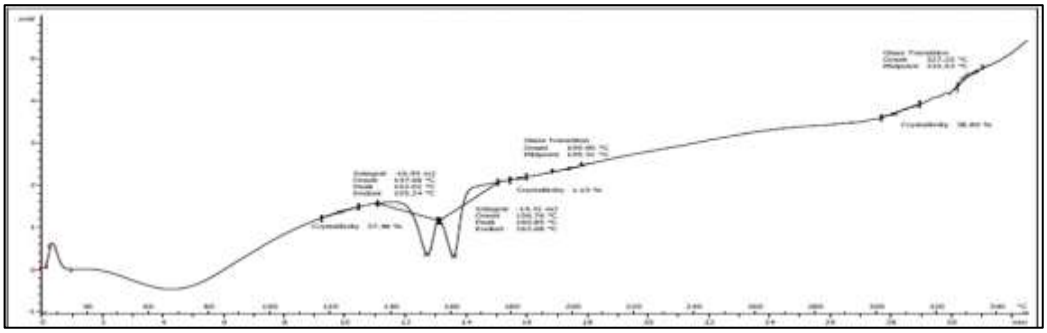

Fig. 7. DSC Thermogram of BSA-LYCOAT RS 720

X-Ray Diffractometry (XRD)

In Fig. 8, 9, and 10, BSA-LYCOAT RS 720 conjugates showed partly amorphous structure as observed from powder X-ray diffraction pattern. The diffractogram of BSA showed characteristics diffraction peaks at 2θ values of 7.368º, 12.280º, and 19.342º indicating crystalline nature. LYCOAT RS 720 showed blunt diffraction peaks at 9.671º and 20.339º indicating amorphous nature. BSA-LYCOAT RS 720 conjugates showed different diffraction peaks of Lycoat RS 720 at 2θ values of 9.62º and 20.418º with less intensity and intensity of BSA peaks decreased instantly showed amorphous nature.

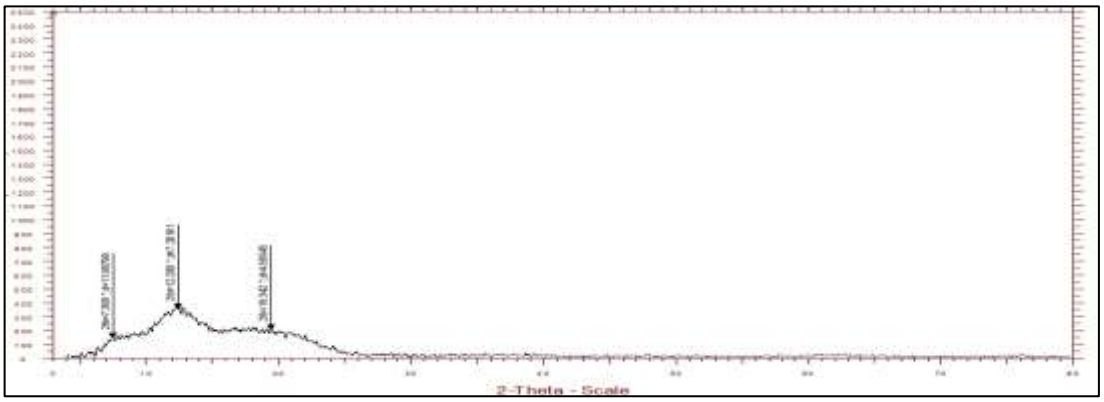

Fig. 8. XRD Pattern of BSA

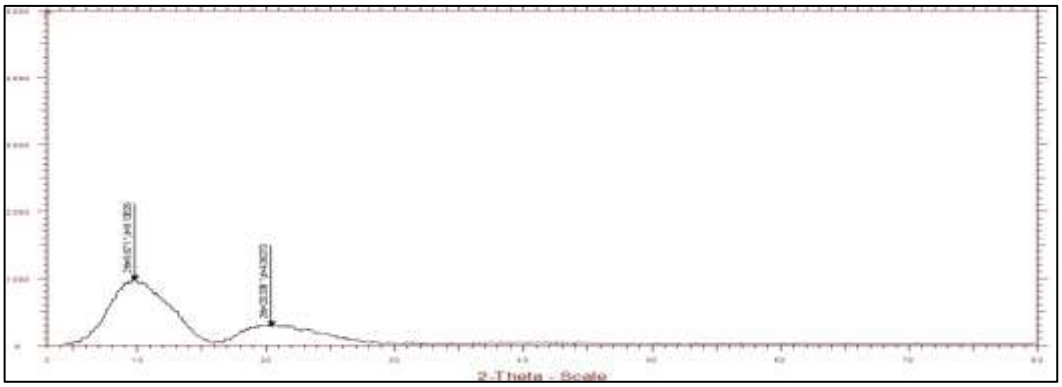

Fig. 9. XRD Pattern of Lycoat RS 720

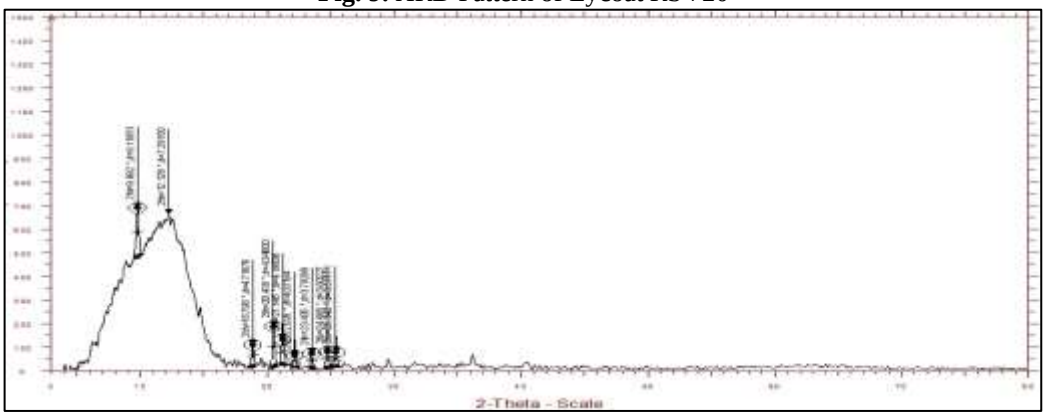

Fig. 10. XRD Pattern of Conjugates

Particle Size and Particle size distribution study

The particle size of the PNs is a fundamental factor because it decides the rate and extent of drug release as well as drug absorption. The smaller particle size offers a larger interfacial surface area for drug absorption and improves the bioavailability. The calculation of polydispersity index takes into account the particle mean size, the refractive index of the solvent, the measurement angle and the variance of the distribution. Low polydispersity index value might be associated with a high homogeneity in the particle population, whereas high polydispersity index values suggest a broad size distribution or even several populations. The optimized formulation batch (F6) showed mean particle size 310 nm before lyophilization while 257 nm after lyophilization with PDI 0.589 and 0.533 respectively as shown in figs.11-12. The MPS and PDI were decreased in freeze-dried powder. This might be due to adherence of cryoprotectant throughout freeze-drying. The optimization of cryoprotectant was based on appearance of cake and ease of reconstitution.

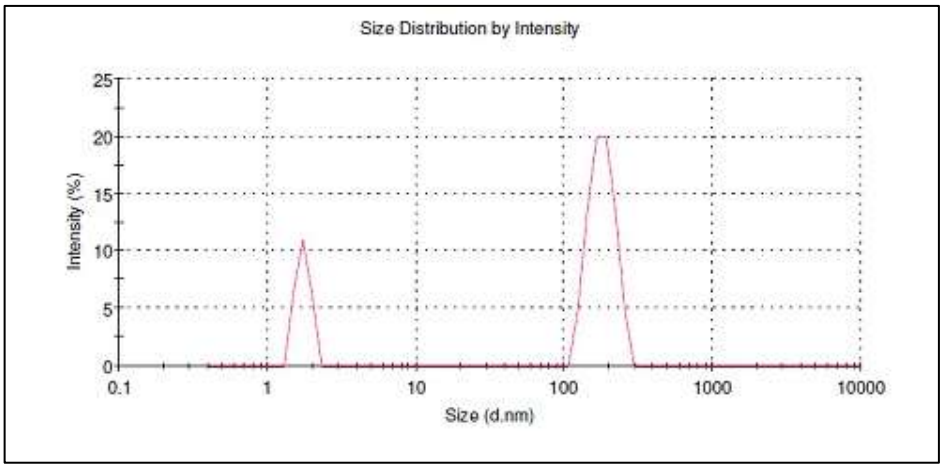

Fig. 11. Particle size of Formulation Batch before Lyophilization (F6)

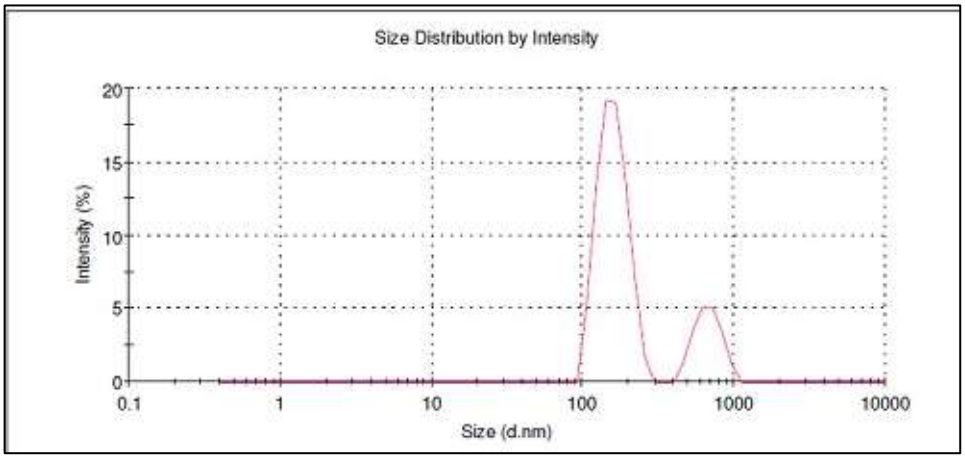

Fig. 12. Particle size of Formulation Batch after Lyophilization (F6)

Zeta Potential Measurement:

The zeta potential values of plain drug, blank nanoparticles and drug loaded nanoparticles that was found to be -10.2 mV, -30.9 mV and -22.4 mV respectively as shown in figs. 13-15.

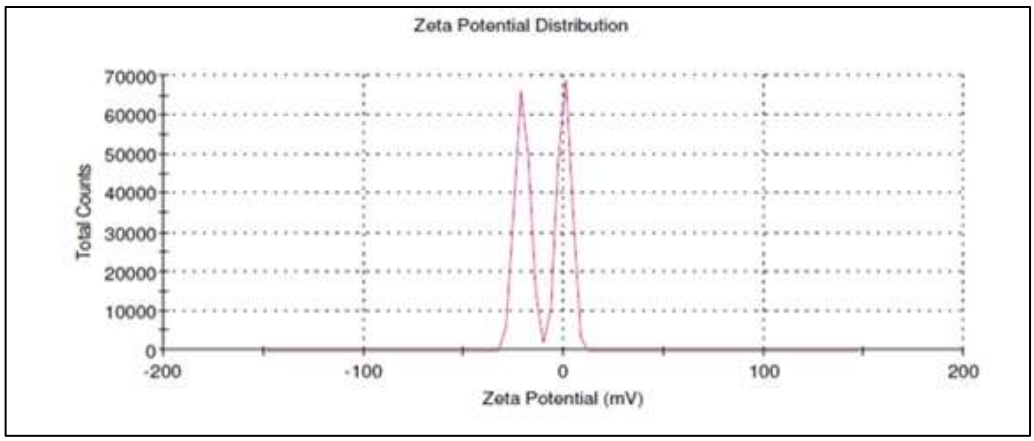

Fig. 13. Zeta Potential of Pure extracts

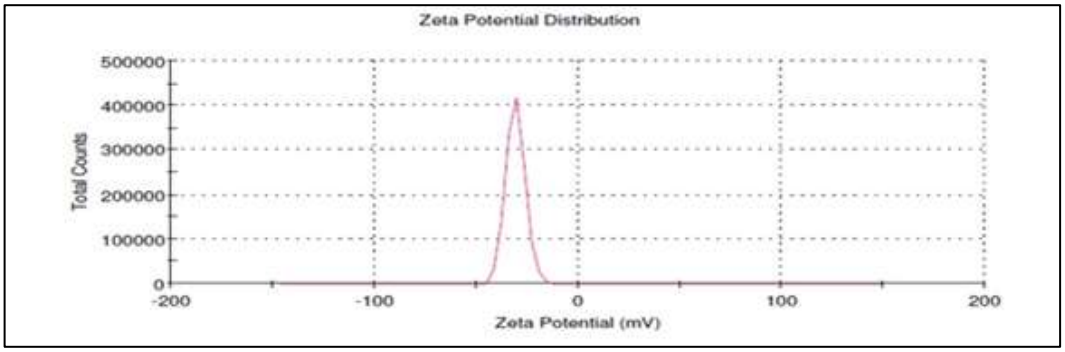

Fig. 14. Zeta Potential of Blank Nanoparticles

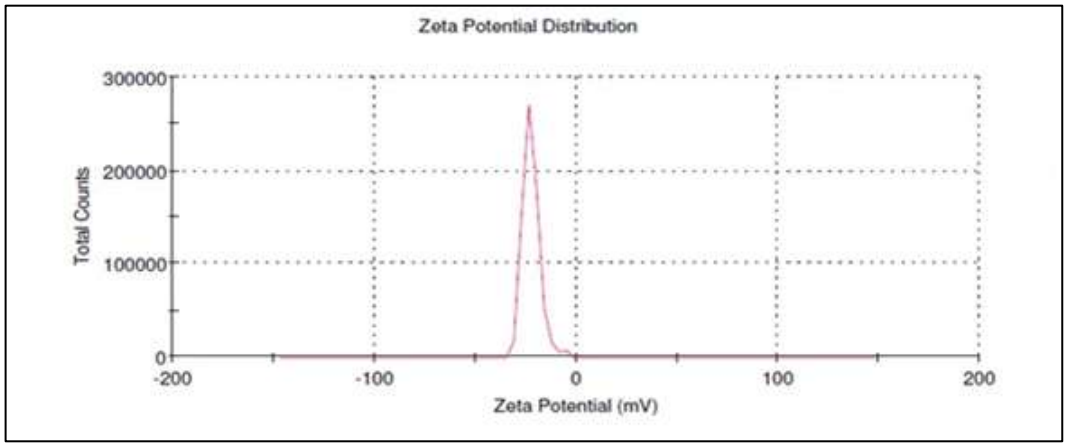

Fig. 15. Zeta Potential of Formulation Batch (F6)

Entrapment efficiency

The % EE depends on the properties of drug and polymer used. Amongst of all batches % EE was good due to solvent evaporation method. The % EE of optimized batch was found to be 88.32 as shown in table 8. From result we concluded, with the increase in the polymer conjugates concentration the entrapment efficiency increases, as more the polymer available more will be the entrapment efficiency.

Table 8. Entrapment Efficiency of Different Formulation Batches

Formulation Batches	Entrapment Efficiency (%)
F1	80.5
F2	80.9
F3	86.6
F4	87
F5	85.32
F6	**88.32**
F7	87.32
F8	80
F9	87

Production Yield

All the batches showed production yield in between 86-96% as shown in table 9. The resultant yield is an indication that the method can be appropriate for technology transfer that is production on large scale.

Table 9. Production Yield of Different batches

Batch Code	Production Yield (%)
F1	86.50±0.18
F2	92.12±0.22
F3	94.50±0.16
F4	93.50±0.14
F5	94.33±0.23
F6	95.66±0.24
F7	95.60±0.22
F8	94.10±0.15
F9	96.80±0.18

Surface Morphological Study (TEM)

Surface morphology of the Polymeric Nanoparticles was evaluated using transmission electron microscope (TEM) from which it can be seen that the nanoparticles have smooth surfaces. Nanoparticles show spherical shape with size 200 nm as shown in fig.16.

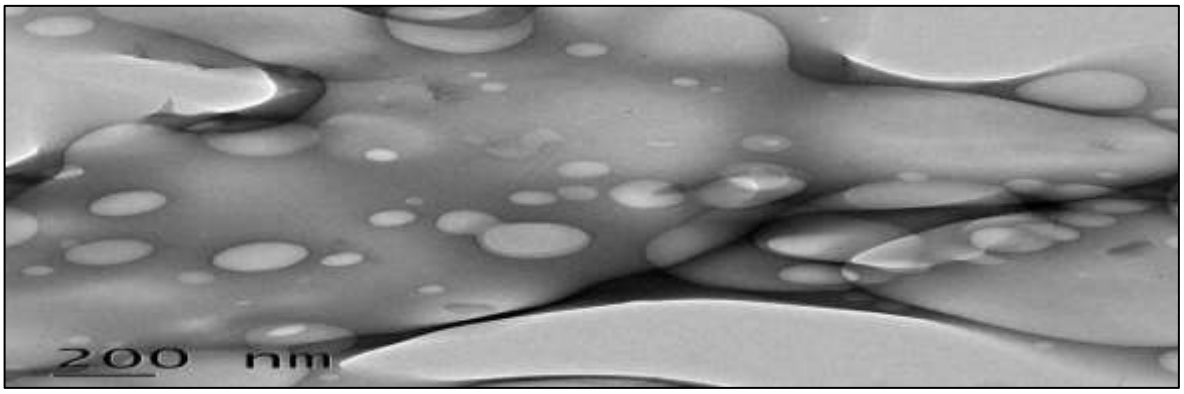

Fig. 16. TEM Image of Formulation Batch (F6)

8) *In-Vitro* Drug Release:

Rhynchosia rothii loaded polymeric nanoparticles of all batches were studied *in-vitro* for drug release. For batches F6, the maximal drug release was found to be about 91-94% as shown in Table 10 and fig.17. The *in-vitro* release of produced polymeric nanoparticles in phosphate buffer saline (PBS) (PH 7.4) at 37ºC was studied. Polymeric nanoparticles were dialyzed for 60 min. The quantity of medication released was measured by using a UV-visible spectrophotometer to measure absorbance

Table 10. *In-vitro* release profile of *Rhynchosia rothii* loaded Nanoparticles

Sr. No.	Time (Min.)	Herbal Nanoparticles (%) (F4)
1	0	0
2	10	27.42
3	20	41.04
4	30	46.62
5	40	61.52
6	50	91.02
7	60	94.24

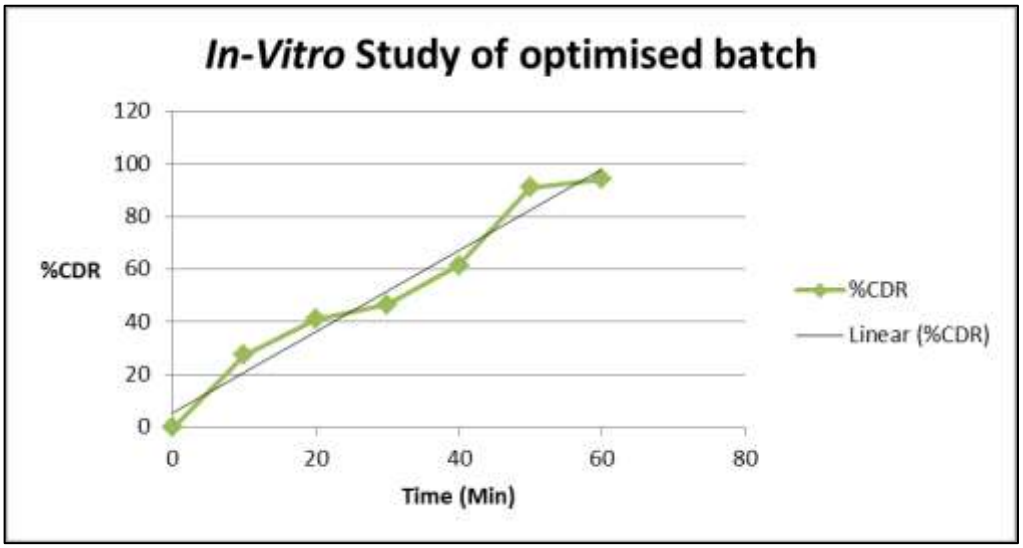

Fig. 17. *In-vitro* drug release of optimized Polymeric Nanoparticle

Stability Study of polymeric nanoparticles:

Accelerated stability studies of formulation were conducted by measurement of particle size, PDI, zeta potential and drug content. Before stability studies, *Rhynchosia rothii* loaded PNPs showed mean particle size 257 nm with PDI 0.533. After stability studies mean particle size and PDI was found to be 261 nm and 0.539 respectively. There were no significant changes in particle size and PDI after three month storage. Zeta potential of optimized formulation before and after stability study was found to be -22.4 and -22.2 mV, respectively. Based on these results it is revealed that,

Rhynchosia rothii loaded PNPs (Formulation batch F6) were found to be stable formulation at the given temperature and humidity condition.

EVALUATION OF OINTMENT

Organoleptic characteristics

Table 11 displays the ointment compositions' organoleptic characteristics, such as their physical appearance, color, texture, phase separation, homogeneity, and initial skin sensation. The ointments had good aesthetic appeal, a smooth texture, and were all homogeneous with no evidence of phase separation, according to the results. Each mixture had an aromatic scent and was white in color.

Table 11. Physicochemical evaluation of ointment formulations

Formulations	Physical appearance	Texture	Phase separation	Homogeneity	Immediate skin feel
F1	Opaque	Rough & Hard	No	Homogenous	No grittiness
F2	Opaque	Smooth	No	Homogenous	Yes grittiness
F3	Opaque	Smooth	Yes	Homogenous	No grittiness
F4	**Opaque**	**Smooth**	**No**	**Homogenous**	**No grittiness**

pH

The pH of all formulations was discovered to be within the acceptable range of 6.80±0.152 and 7.02±0.174, which is shown in Table 12. All formulas' pH values fall within the skin's typical pH range.

Viscosity

All of the formulations' viscosities were recorded and discovered to range between 2314±6.13 and 2851±9.93 CPS at 10 rpm, as indicated in Table 12. Each and every composition displayed pseudo-plastic flow. Three readings were averaged, and the standard deviation was calculated (n=3).

Spreadability

Three categories of ointment spreadability exist: low, moderate, and high. Following screening, it was discovered to be directly inversely related to the volume of liquid parafin. The ointment grew thinner and more spreadable when the amount of liquid paraffin was increased. All formulations' spreadabilities were assessed, and it was found that formulation F4 spreads more readily than the other formulations in Table 12.

Table 12. Evaluation parameters of ointment formulations

Formulations	pH (mean±SD)	Viscosity at 10 rpm (CPS) (mean±SD)	Spreadability g.cm/s (mean±SD)	Water number (mean±SD)
F1	6.80±0.152	2851±9.93	80.00±3.83	1.2±0.25
F2	7.01±0.185	2612±8.13	109.09±5.13	1.3±0.08
F3	6.90±0.189	2472±7.23	112.57±4.23	1.3±0.12
F4	**6.92±0.244**	**2412±8.03**	**110.16±3.53**	**1.4±0.10**

Stability study

According to ICH requirements, a stability study was conducted on each ointment formulation, and the findings are displayed in Table 13. For the duration of the stability studies, the formulations' appearance was clear and there was no appreciable change in the pH, spreadability, or viscosity of the optimized formulation.

Table 13. Evaluation parameters of ointment formulations

Formulations	pH (mean±SD)	Viscosity at 10 rpm (CPS) (mean±SD)	Spreadability g.cm/s (mean±SD)
F4			
Before Stability Study	6.59±0.96	2470±6.96	102.91±4.12
After Stability Study	6.79±0.12	2470±06.23	102.25±3.20

The prepared ointment formulations were evaluated using a variety of criteria, and the results were within the set limits, which are shown in Tables 11 to 13. All of the formulations were discovered to have an alkaline pH. In comparison to previous formulations and prototype formulations, formulation F4 has a higher spreadability. It can be seen that lowering the concentration of was improved spreadability overall. Based on the spreadability, viscosity, and water number results, the formulation F4 made with paraffin wax was chosen as the best formulation. According to a stability analysis, the improved formulation is stable for a month.

CONCLUSION

Following the ointment formulation, *Rhynchosia rothii* loaded Lycoat RS 720-BSA conjugated polymeric nanoparticles were added. Maillard Reaction was used to develop the Lycoat RS 720-BSA conjugate. The solvent evaporation approach was used to create nanoparticles with *Rhynchosia rothii* loaded on them. The nanoparticles had a 257nm particle size and exhibited a spherical shape. The zeta potential in the formulation was -22.4 mV. The *Rhynchosia rothii* extract was created as an absorbent ointment formulation with a pH of 6.80–6.92 and a spreadability of 80.00–110.16 g.cm/s. It also has a distinctive aroma. Ointment containing herbal nanoparticles from the F4 batch has produced positive results. It was observed that the ointment containing the active ingredient of paraffin wax had good strength, viscosity, and spread ability. It is hoped that this work would spur additional investigation into and belief in the use of natural active components in medications. A new method of promoting nanoparticles in herbal medication delivery systems is by employing them in nanoparticles and an ointment.

Conflict of Interest

Authors declared that there are no conflicts of interest exists.

Acknowledgement

None

Competing Interests

Authors have declared that no competing interests exist

REFERENCES

1. Rawlings AV, Harding CR. Moisturization and skin barrier function. Dermatol Ther 2004;17(1)1:43-8.
2. Marty JP. NMF and cosmetology of cutaneous hydration. Ann Dermatol Venereol 2002;129(1):131-6.
3. Cravello B, Ferri A. Relationships between skin properties and environmental parameters. Skin Res Technol 2008;14(2):180-6.
4. Cancalon P. Chemical composition of sunflower seed hulls. J Am Oil Chem Soc 1971;486(12):29-32.
5. Nikam, A.P., Mukesh, P.R. and Haudhary, S.P. Nanoparticles—an overview. J. Drug Deliv. Ther, 2014;3(1):1121-1127.
6. Jawahar, N. and Meyyanathan, S.N. Polymeric nanoparticles for drug delivery and targeting: A comprehensive review. Int. j. health allied sci. 2012;1(4):217-223.
7. Abhilash, M. Potential applications of Nanoparticles. Int J Pharm Bio Sci. 2010;1(1):7-9.
8. Nagavarma, B.V.N., Yadav, H.K., Ayaz, A., Vasudha, L.S. and Shivakumar, H.G. Different techniques for preparation of polymeric nanoparticles-a review. Asian J. Pharm. Clin. Res, 2012;5(3):16-23.
9. Smith, A.A., Zuwala, K., Pilgram, O., Johansen, K.S., Tolstrup, M., Dagnæs-Hansen, F. and Zelikin, A.N. Albumin–polymer–drug conjugates: long circulating, high payload drug delivery vehicles. ACS Macro Letters, 2016;5(10):1089-1094.
10. Edelman, R., Assaraf, Y.G., Levitzky, I., Shahar, T. and Livney, Y.D. Hyaluronic acid-serum albumin conjugate-based nanoparticles for targeted cancer therapy. Oncotarget, 2017;8(15):24337-24353.
11. Ratnayake, W.S., Hoover, R. and Warkentin, T. Pea starch: composition, structure and properties-a review. Starch-Stärke, 2002;54(6):217-234.
12. Suryawanshi MV, Mahajan HS. Formulation and Characterization of Betulinic Acid Loaded Polymeric Nanoparticles for the Treatment of Breast Cancer. IJARW. 2019;1(10):15-27.
13. Rammohan A, Reddy GM, Bhaskar BV, Gunasekar D, Zyryanov GV. Phytochemistry and pharmacological activities of the genus Rhynchosia: a comprehensive review. Planta. 2020;251(1):1-5.
14. Mary JL, Raghavendra NM, Subrahmanyam CV. Antidiabetic and Antioxidant activity of Rhynchosia beddomei baker. Int J Med Res Rev. 2014;2(1):1323-32.
15. Rawat M, Singh D, Saraf S. Nanocarriers: Promising Vehicle For Bioactive Drugs. Biol. Pharm. Bull. 2006;29(1):1790-8.
16. Ansel. Pengantar Bentuk Sediaan Farmasi Edisi IV. Jakarta: UI Press; 2005.
17. Tayade, S. D., & Silawat, N. (2021). Phytochemical Screening and Wound Healing Activity of Different Leaf Extracts of Rhynchosia rothii in Rats. "J. Pharm. Res. Int. 33(46B), 386-393.
18. Sharma PP. Cosmetics-formulation, Manufacturing and Quality Control, Delhi, India: Vandana Publications; 2014;7(5)181-91.
19. Pawar A, Singh S, Rajalakshmi S, Shaikh K, Bothiraja C. Development of fisetin-loaded folate functionalized pluronic micelles for breast cancer targeting. Artif Cells Nanomed Biotechnol. 2018;46(sup1):347-61.
20. Cavazzuti, M., 2013. Design of experiments. In Optimization Methods (pp. 13-42). Springer Berlin Heidelberg.
21. Qi J, Yao P, He F, Yu C, Huang C. Nanoparticles with dextran/chitosan shell and BSA/chitosan core—doxorubicin loading and delivery. Int. J. Pharm. 2010;393(1-2):177-85.
22. Zhao L, Du J, Duan Y, Zhang H, Yang C, Cao F, Zhai G. Curcumin loaded mixed micelles composed of Pluronic P123 and F68: preparation, optimization and in vitro characterization. Colloids and Surfaces B: Biointerfaces. 2012;97(1):101-8.
23. Mahajan HS, Mahajan PR. Development of grafted xyloglucan micelles for pulmonary delivery of curcumin: in vitro and in vivo studies. Int. J. Biol. Macromol. 2016;82(1):621-7.
24. Bothiraja C, Rajput N, Poudel I, Rajalakshmi S, Panda B, Pawar A. Development of novel biofunctionalized chitosan decorated nanocochleates as a cancer targeted drug delivery platform. Artif Cells Nanomed Biotechnol. 2018;46(sup1):447-61.
25. Bronze-Uhle ES, Costa BC, Ximenes VF, Lisboa-Filho PN. Synthetic nanoparticles of bovine serum albumin with entrapped salicylic acid. Nanotechnol. Sci. Appl. 2017;10(1):11.
26. Taralkar SV, Chattopadhyay S. A HPLC Method for determination of ursolic acid and betulinic acids from their methanolic extracts of Vitex Negundo Linn. J. Anal. Bioanal. Tech. 2012;3(3):1-6.
27. Madane RG, Mahajan HS. Curcumin-loaded nanostructured lipid carriers (NLCs) for nasal administration: design, characterization, and in vivo study. Drug deliv. 2016;23(4):1326-34.
28. Sahib MN, Abdulameer SA, Darwis Y, Peh KK, Tan YT. Solubilization of beclomethasone dipropionate in sterically stabilized phospholipid nanomicelles (SSMs): physicochemical and in vitro evaluations. Drug Des. Devel. 2012;6(1):29-42.
29. Costa P, Lobo JM. Modeling and comparison of dissolution profiles. Eur J Pharm Sci. 2001;13(2):123-33.
30. Jain S, Mittal A, K Jain A, R Mahajan R, Singh D. Cyclosporin A loaded PLGA nanoparticle: preparation, optimization, in-vitro characterization and stability studies. Curr. Nanosci. 2010;6(4):422-31.
31. Lachman L, Herbert AL, Joseph LK. The Theory and Practice of Industrial Pharmacy, Chp 3. India: Varghese Publication House; 1999;569.
32. Kilor V, Sapkal N, Vaidya G. Design and development of novel microemulsion based topical formulation of hesperidin. Int J Pharm Pharm Sci. 2015;7:142-8.
33. Multimer M. Spreadability determination by an apparatus. J Am Pharm Assoc. 1956;45:212-4.

34. Dua D, Srivastava NS. Study on antioxidant and anti-aging properties of few medicinal plants. Int J Pharm Pharm Sci. 2016;8:344-7.
35. Ayobami OO, Okikiolu OJ, Hannah OO, Samuel OO. Ocular tolerance and in-vitro release of chloramphenicol in prospective eye ointment bases. Int J Pharm Pharm Sci. 2015;7:306-11.
36. Daniels R, Knie U. Galenics of dermal products vehicles, properties and drug release. J Dtsch Dermatol Ges. 2007;5:367-83.
37. Suchiwa PO, Soravoot R, Ounaroon A, Kongkaew C, Tiyaboonchaia W. Development, characterization and skin irritation of mangosteen peel extract solid dispersion containing clay facial mask. Int J Appl Pharm. 2018;10:202-8.